

Interface effect between blue phosphorus and metals

Si-Cong Zhu,^{*a, b} Tie-Yi Hu,^a Cho-Tung Yip,^c Kai-Lun Yao^d and Chi-Hang Lam^{*b}

^a The State Key Laboratory for Refractories and Metallurgy, Hubei Province Key Laboratory of Systems Science in Metallurgical Process, Collaborative Innovation Center for Advanced Steels, International Research Institute for Steel Technology, Wuhan University of Science and Technology, Wuhan 430081, China

^b Department of Applied Physics, Hong Kong Polytechnic University, Hung Hom, Hong Kong, China.

^c School of Science, Harbin Institute of Technology (Shenzhen), Shenzhen, China

^d Wuhan National High Magnetic Field Center and School of Physics, Huazhong University of Science and Technology, Wuhan 430074, China

Email: sczhu@wust.edu.cn (Si-Cong Zhu) C.H.Lam@polyu.edu.hk (Chi-Hang Lam)

Abstract

The contacted properties of metal substrates with single layer (monolayer) blue phosphorus are calculated by first principles. We analyze the charge transfer, atomic orbital overlap, electronic properties and potential barrier at the interface of metal contacted blue phosphorene (BlueP) to understand how to effectively inject electrons from the metal into the contacted blue phosphorus. We inquire into interfacial effect of blue phosphorene directly in contact with five representative metallic substrates-Au (111), Ag(111), Al(111), Co(111) and Sc(0001), which are having minimal lattice mismatch with the BlueP. We find that the contact properties of these five metals are ohmic contact and schottky contact. Of the five different contact metals, Co-BlueP heterojunction has the best electrical conductivity. The lower SBH in the Al contact can also lead to a good substrate for a Schottky contact for the heterojunction. These results can provide guidance for the future design of BlueP-based electronic devices and for the exploration of new low-dimensional semiconductor transport processes.

Keywords: First Principles, blue phosphorene, Schottky contact, electronics, heterojunction

Introduction

Various two-dimensional (2D) crystals such as silicene[1], graphene[2], germanene[3, 4], transition metal dichalcogenides(MoS₂, MoSe₂, WSe₂, etc.)[5, 6],

phosphorene [7-12], are being actively studied for the post-Si nanoelectronics era, for their promise of aggressive channel length scalability and reduced short channel effects. Layered black phosphorus is emerging as a viable contender in the competitive field of 2D semiconductors with fabricated FET's achieving ON and OFF current about 10^4 ratio and $1000 \text{ cm}^2/\text{Vs}$ field effect mobility [13-15]. Layered blue phosphorus, previously described as the A7 phase [17, 18], has been showed to be as stable as black phosphorus but should have a different electronic structure [16]. Interestingly, the electronic band structures of the two allotropes are significantly different. One layer BlueP has an indirect band gap of $\sim 2.0 \text{ eV}$ while one layer black phosphorous has an intrinsic direct band gap of $\sim 1.0 \text{ eV}$ at the Γ point [22, 25]. Recently, Zhang[20] developed a MBE process that uses black phosphorus as the precursor and epitaxial growth of single layer BlueP on Au(111). The discovery of large-scale, high-quality atomic lamellar blue phosphorus epitaxial growth could lead to the rapid development of new electronic and optoelectronic devices based on this emerging two-dimensional material.

For black phosphorus [21], carbon nanotubes [22], graphene [23], transition metal dihalides [24], phosphorene [25] and other new nanomaterials, people have invested a lot of theoretical and experimental research to understand their contact characteristics with metals. On the other hand, metal-BlueP contact has not been studied systematically at present. In particular, our goal is to identify metal-BlueP contacts as ohmic or schottky contact to realize their full potential in the future as a new and emerging electronic material.

In our work, we use the first principles density functional theory calculations to screen out Au, Ag, Al, Co, and Sc, which are commonly used to evaluate the ohmic and schottky properties of the metal-BlueP interface. Firstly, we obtain the optimal interlayer separation by refer to the traditional binding energy calculation. Eventually, it is observed that among these five metals, Co possesses minimum barrier potential, the maximum electron density, maximum orbital overlap and provides the best contact properties leading to an ohmic contact, which is the best for carrier injection; while Al and Au result in a Schottky contact.

Methods

We do all the calculations using the density functional theory (DFT) of the Atomistix ToolKit (ATK). Our calculation is based on the traditional kohn-sham [26], using local density approximation (LDA) -PZ implemented in Atomistix ToolKit[27] (ATK). The

optimized lattice constants for BlueP is $a=b=3.33 \text{ \AA}$ [21]. We also use general gradient approximation (GGA) - Perdew-Burke-Ernzerhof (PBE) to calculate, and the results show that it is similar to the previous ones. A Double ζ polarization is set to expand on the basis of electron density. Sample $8 \times 8 \times 3$ k points in the contact area of Brillouin zone (BZ). In the process of geometric optimization, the density grid cut off is 150 Rydberg, and the maximum force is 0.05 eV \AA^{-1} . We use a supercell which contains six layers of metal atoms that are connected to the surface of $m \times n$ unit cells BlueP. A vacuum area of approximately 10 \AA is maintained above the BlueP to avoid pseudo-interactions due to periodic boundary conditions.

Results and discussion

In terms of the process robustness and electrical reliability, bulk metal contacts form the main strategy for BlueP. Metals with suitable physical properties (e.g. electrical conductivity, melting point, and thermal conductivity) as well as chemical properties (e.g. toxicity and stability) for contact applications include Al, Au, Ag, Cu, Cr, Pd, In, Co, Sc, Pt, Mo and Ti. The lattice of metal may play an important role in the BlueP-metal system. After the metal and semiconductor match, we keep the metal lattice unchanged, and only change the lattice constant of the two dimensional blue phosphorus, which is consistent with the metal lattice constant. Therefore, if the lattice constants of the metal and the blue phosphorus differ greatly, the strain on the blue phosphorus will increase, which will directly affect the electronic structure properties of the blue phosphorus. So we only chose metals whose lattice constant mismatch was less than 0.5%. To design the metal/BlueP contacts, we consider metals that will well match the BlueP by having a lattice plane. We can exclude Ti, Cr, Cu, Pd, Ni, In and Pt due to the large lattice constant misfit with BlueP, which may lead to unstable structures or small orbital overlaps. After going through all metals about the lattice constant, we find that Au(111), Ag(111), Al(111), Co(111), Sc(0001) and Mo(111) cover a wide range of work functions, and they are suitable candidates for the metal/BlueP contacts. Their Initial configurations are based on the structure of bulk metals and are similar for Au (111), Ag (111) and Al (111) but distinct for Co (111), Sc (0001) and Mo(111). In this work, we do not constraints any layer of metals from the interface to emulate the effect of layers in modeling. The optimized metal/BlueP structures are shown in Figure 1(a)-(c). We know that metal/BlueP form similar structures with Au(111), Ag(111), Al(111). Co(111) and Sc(0001) surfaces

when there are no significant P-P bond distortions. The interactions between P and Mo atoms are very strong, and as a result, the structure of Mo contacted BlueP cease to be periodic because of the broken P-P bonds. So we're not going to list any Mo contact structure information in the manuscript. The calculated work functions, binding energies, and equilibrium bonding lengths for the stable metal/BlueP structures are generalized in the Table I. d_z is denoted the average distance between BlueP layer and the substrate along the z axis. The metal /BlueP binding energy of each unit is used to characterize its contact strength which is defined by $E_b = (E_{\text{BlueP}} + E_{\text{sub}} - E_{\text{BlueP-sub}})/n$, where E_{sub} and E_{BlueP} are the total energies of substrate and BlueP, while $E_{\text{BlueP-sub}}$ is the total energy of BlueP absorbed on substrate, respectively. All energies are acquired from totally optimized structures. Also, n is denoted the number of BlueP unit cells in the heterojunction. Only BlueP is strained in planar directions to match the surface of the metals. Among the studied contacts, Co/BlueP has the smallest $d_z = 1.89\text{\AA}$, the smallest BlueP planar strain = 0.85%, and the maximum binding energy $E_b=3.184\text{eV}$. The smallest d_z is produced because each P atom of BlueP bonds more to two or more Co atoms than any other metal. This strongly indicates good metal/BlueP contact properties.

In the following part, we quantify the properties of the metal/BlueP contacts using partial density of states (PDOS) as shown in Figure 2. In contrast, the PDOS of BlueP have a metallic character. A detailed PDOS analysis reveals that the states are predominantly of P p-orbital character close to Fermi level E_f . Essentially, Figure 2 shows more P p-states than P s-states at energy levels corresponding to the band gap of phosphorene. The band structure [Figure 5(a)] of freestanding BlueP has a gap around the Fermi level. The gap regions are slightly shifted when we apply the strain in Table 1 appropriate for the contacts without actually introducing the contacts themselves. In Figure 2(a)-(e), the regions shaded in white indicates levels between the conduction band edge (E_c) and the valence band edge (E_v) for free-standing phosphorene under strain given in Table 1. The band structure and partial density of states (PDOS) obtained by DFT calculation confirm the metallization of BlueP under metal contact. As shown in Figure 5(b) (c), most of the contacted BlueP (excluding metals) bands (red) are modified by the metal contact, a new band (gray) is formed, extending to the original band gap. We also list the values of the original BlueP conduction band minimum (CBM) and valence band maximum (VBM) relative to Fermi energy levels, as shown in Table 1. Only the cases of Ag, Au and Al lead to n-type behavior, as indicated by the CBM being less than the VBM (see the table 1).

The position of E_f is slightly closer to the conduction band edge (E_c) than the valence band edge (E_v) in Figure 2(a)-(c). The E_f of Co/BlueP contacts is located in the middle of the BlueP band gap [Figure 2(d)]. We observed that the Fermi levels of all heterojunctions except for the case of Sc move up about 0.13 eV to 0.2 eV with respect to the bottom of the conduction band for the freestanding BlueP. The PDOS is much larger for Co/BlueP and Al/BlueP [Figure 2(d) (c)] near the Fermi level than that of the other contacts, because of the contribution of the p states increases significantly. Since the Co/BlueP bonding distance d_z (see table I) is obviously smaller than the other bonding distance d_z , the p states of p atom interacts more strongly with the 3d states of Co. In result, Co/BlueP is a better substrate than the others, As a result of good device contacts should be maximally overlapped between the states of either side of the contact interface. Because of lack d electrons, the Al/BlueP with the second largest PDOS at E_f obviously has different electronic structures as will be explained later.

To describe interface charge distribution, Figure 3 plots electron density (ρ) and electron localization function (ELF) for Co, Sc, Ag Al and Au.

From Figure 3(a)-(c) IV, the three structures show no interface barrier which result in Ohmic contacts. The averaged electron densities of plotted along z-direction are shown in I and II of Figure 3(a)–(c). The minimum value for electron density at the interface is 0.019\AA^{-3} for Sc contact. This small value of minimum electron density indicates weak bonding with BlueP. In contrast, a high value of 0.045\AA^{-3} is obtained in order for Co to exhibit strong covalent bonds, resulting in low resistance contact. The value of 0.020\AA^{-3} for Ag is only slightly more in comparison to that for Sc and this indicates bond strength similar to that for the case of Sc.

The effective potential (EP) of an electron represents its interaction with the ion nucleus and other electrons. The interface tunneling barrier is calculated as the difference between metal atomic potential and metal /BlueP interface gap potential. To further analyze the contact properties, we investigate the effective potential and examine the existence of any barrier at the semiconductor/metal interface. The results are in IV of Figure 3(a)-(c). There is no barrier at the interface, so the three structures are all Ohmic contact. On the other hand, Co/BlueP contacts have a higher electron density at the interface and thus result in higher electron injection efficiency than in the cases of Sc/BlueP and Ag/BlueP. Furthermore, the electron localization functions for the contacts are also shown in III of Figure 3(a)-(c). The ELF at the Co/BlueP interface [Figure 3(a) III] is larger than those of the other heterojunction, indicating a

larger overlap of electron orbits between BlueP and metal. For more clearly seen, we plot cross-section of the ELF between the phosphorus atom and its nearest metal atom is shown in Figure 4 (a)–(e). The distance between such a P–M pair is the shortest one, and this is the position with the strongest interaction between the metals and BlueP layer. For the Ohmic contact Co/BlueP(a), Sc/BlueP(b) and Ag/BlueP(c), the orbital overlaps between Co-P are more efficient than Ag-P, the ELF at the Co-P interface is higher. For Sc-P pair, scandium atom shows the much more blue region which signifies the electrons of scandium atom with almost no localization and forms metallic bonds with other scandium atoms. In the issue, Co/BlueP is a better heterojunction than the other contact structures in Ohmic contact. The electron states at the conduction band-edge of Co/BlueP mainly from the metal d-orbits. Therefore, it is believed that the d orbital can be hybridized with the electron orbital in the phosphorus atom to obtain a better electron injection and thus form a lower contact resistance.

Similar analysis for Al and Au are shown in Figure 3(d), (e). The Al and Au contacts exhibit finite potential barriers [see panel IV], implying Schottky rather than Ohmic contacts. The Al/BlueP contact region has an electron density of about 0.025 \AA^{-3} as shown in Figure 3(d) (II) and an electron tunneling barrier of 0.04 eV from Figure 3(d) (IV). Although the Au/BlueP contact region has a less favorable electron density of about 0.02 \AA^{-3} [Figure 3(e) (IV)], it has a smaller tunneling barrier of 0.01eV [Figure 3(e) (IV)]. The Al and Au contacts are thus comparable in quality. In Figure 4, for the schottky contact Al/BlueP(d) and Au/BlueP(e), the orbital overlaps between Al-P are more efficient than Au-P, the ELF at the Al-P interface is higher than Au-P one. The Al/BlueP has a much higher electron density compared with the Au/BlueP contact, and allows the increasing electron injection efficiency. And as shown in Figure 3(d) II and 3(e) II, the Al/BlueP has a much higher electron density compared with the Au/BlueP contact, and allows the increasing electron injection efficiency. These also can be explained by the Schottky barrier.

Schottky barrier height (SBH) is another key factor in determining the contact resistance of semiconductor devices. The metalized BlueP hetrojunction is confirmed by the DFT calculation. In Figure 5, only the Schottky contact systems are plotted in gray curve. In addition, the optimized BlueP band structure (red curve) without contacted metal is drawn and superimposed on the new band structure (gray curve) to align the old and new subbands for reference. Then measured the corresponding Φ_{SB} is in each plot. From DFT simulation results, the Schottky Barriers are 0.78eV and

0.82eV for Al/BlueP and Au/BlueP respectively, as shown in Figure 5(b)-(c). Using this method, all the contact structure Φ_{SB} calculated are also listed in table 1.

Besides, in Al/BlueP contact, Fermi energy level is only pinned at 0.78eV below the eigen BlueP original conduction band (Table 1), indicating the Schottky barrier height is 0.78eV(n-type contact) at the interface a little lower than Au/BlueP. It is important to note that the electrons in the overlapping states of the Al/BlueP system are not localized, which leads to better electron injection, and it should be forming lower contact resistance than the other Schottky contacts.

The charge population of the blue phosphorus and metal atoms are acquired from the Mulliken population analysis (in Table 2). The charge transfer for Co/BlueP is the largest among the Ohmic contacts, which implies that stronger ionic bonds are formed in the interfaces than the other metal contacts. The bond length decreases with the Mulliken charge transfers of P atoms. The shortest bond length between Co with Phosphorus is 2.182 Å. Based on the above analyses, the charge transfer of the BlueP interface was studied, Co/BlueP is an excellent Ohmic contact while the low resistance is caused by delocalized 3d and 2p electrons. The strong valence bond leads to bigger electrons orbital overlap, so the Co contact has a lower resistance. For the schottky contact, the Al heterojunction show higher values of charge transfer, and these can well explain our previous results. For both contacts, the charge populations of Co-P bonds at the interfaces can be even higher than those of Al-P bonds, and this implies stronger ionic bonds at the interfaces.

Summary

In summary, we study theoretically the electronic and structural response of metal/BlueP contacts via DFT calculations. We only consider metals giving rise to small strains when contacted with BlueP. Also, the optimized heterojunction must be not strongly distorted the P-P bond. We have found that five metals surfaces, namely Al (111), Ag (0001), Au (111), Co (111) and Sc (0001) satisfy these conditions. We predict that BlueP absorbed on these metals form viable metal/BlueP heterojunction. Comparing the optimized lattice structure, charge transfer, density of states, electron localized function, potential barrier and band structure at each interface of metal/BlueP, we predict that Co/BlueP exhibits an excellent Ohmic contact compared to the other three metal (Ag, Sc, Co) structures. As a consequence, we conclude that Co (111) is the best choice as a metal substrate for electronic device applications of BlueP. In contrast, Al and Au result Schottky contacts which the electronic potential

barriers are larger than those for the Ohmic contacts. The lower SBH in the Al contact can also lead to a good substrate for a Schottky contact for the 2D material.

Acknowledgements

The authors would like to acknowledge the support from Hong Kong Scholars Program No. XJ2016007, National Natural Science Foundation of China under Grants No. 11704291, No.11647047 and No. 11704292, the HK PolyU under Grant No. G-YBHY, the Foundation for University Key Teachers from the WUST of No. 2017xz024, and the Nature Science Foundation of Hubei Province of No. 2017CFB148.

References

- [1] A.K. Geim, K.S. Novoselov, The rise of graphene, in: *Nanoscience and Technology: A Collection of Reviews from Nature Journals*, World Scientific, 2010, pp. 11-19.
- [2] K. Takeda, K. Shiraishi, *Physical Review B*, 50 (1994) 14916.
- [3] E. Bianco, S. Butler, S. Jiang, O.D. Restrepo, W. Windl, J.E. Goldberger, *Acs Nano*, 7 (2013) 4414-4421.
- [4] S. Cahangirov, M. Topsakal, E. Aktürk, H. Şahin, S. Ciraci, *Physical review letters*, 102 (2009) 236804.
- [5] M. Chhowalla, H.S. Shin, G. Eda, L.-J. Li, K.P. Loh, H. Zhang, *Nature chemistry*, 5 (2013) 263.
- [6] X. Xu, W. Yao, D. Xiao, T.F. Heinz, *Nature Physics*, 10 (2014) 343.
- [7] Y. Ren, P. Liu, F. Cheng, G. Zhou, *Journal of Physics: Condensed Matter*, 30 (2018) 395303.
- [8] Y. An, Y. Sun, M. Zhang, J. Jiao, D. Wu, T. Wang, K. Wang, *IEEE Transactions on Electron Devices*, 65 (2018) 4646-4651.
- [9] M. Zhang, Y. An, Y. Sun, D. Wu, X. Chen, T. Wang, G. Xu, K. Wang, *Physical Chemistry Chemical Physics*, 19 (2017) 17210-17215.
- [10] Y. An, Y. Hou, H. Wang, J. Li, R. Wu, T. Wang, H. Da, J. Jiao, *Physical Review Applied*, 11 (2019) 064031.
- [11] S.K. Das, K. Das, N. Vadakkayil, S. Chakraborty, S. Paul, *Journal of Physics: Condensed Matter*, (2020).
- [12] S. Soleimanikahnoj, I. Knezevic, *Physical Review Applied*, 8 (2017) 064021.
- [13] L. Li, Y. Yu, G.J. Ye, Q. Ge, X. Ou, H. Wu, D. Feng, X.H. Chen, Y. Zhang, *Nature nanotechnology*, 9 (2014) 372.
- [14] H. Liu, A.T. Neal, Z. Zhu, Z. Luo, X. Xu, D. Tománek, P.D. Ye, *ACS nano*, 8 (2014) 4033-4041.
- [15] S.P. Koenig, R.A. Doganov, H. Schmidt, A. Castro Neto, B. Oezylmaz, *Applied Physics Letters*, 104 (2014) 103106.
- [16] Z. Zhu, D. Tománek, *Physical review letters*, 112 (2014) 176802.
- [17] J.C. Jamieson, *Science*, 139 (1963) 1291-1292.

- [18] S.E. Boulfelfel, G. Seifert, Y. Grin, S. Leoni, *Physical Review B*, 85 (2012) 014110.
- [19] J. Guan, Z. Zhu, D. Tománek, *Physical review letters*, 113 (2014) 046804.
- [20] J.L. Zhang, S. Zhao, C. Han, Z. Wang, S. Zhong, S. Sun, R. Guo, X. Zhou, C.D. Gu, K.D. Yuan, *Nano letters*, 16 (2016) 4903-4908.
- [21] S. Zhu, Y. Ni, J. Liu, K. Yao, *Journal of Physics D: Applied Physics*, 48 (2015) 445101.
- [22] Z. Chen, J. Appenzeller, J. Knoch, Y.-m. Lin, P. Avouris, *Nano letters*, 5 (2005) 1497-1502.
- [23] G. Giovannetti, P. Khomyakov, G. Brocks, V.v. Karpan, J. Van den Brink, P.J. Kelly, *Physical review letters*, 101 (2008) 026803.
- [24] I. Popov, G. Seifert, D. Tománek, *Physical review letters*, 108 (2012) 156802.
- [25] J. Li, X. Sun, C. Xu, X. Zhang, Y. Pan, M. Ye, Z. Song, R. Quhe, Y. Wang, H. Zhang, *Nano Research*, 11 (2018) 1834-1849.
- [26] F.M. Bickelhaupt, E.J. Baerends, *Reviews in computational chemistry*, (2000) 1-86.
- [27] M. Khazaei, S.U. Lee, F. Pichierri, Y. Kawazoe, *ACS nano*, 2 (2008) 939-943.

Table captions

Table 1. Calculated supercell, applied strain in the BlueP(%), metal surface direction, equilibrium interface distance (d_z), binding energy (E_b), work function (W_F) of isolated metals, work function (WF) of heterojunction, conduction band minimum (CBM), and valence band maximum (VBM) at metal-blue phosphorus interfaces. And the lattice type, lattice constant and surface lattice length of the five metals.

	BlueP	Ag	Au	Al	Co	Sc	Ni
Super cell		3×2	3×2	3×2	2×2	2×2	2×2
Strain		0.32%	0.2%	0.27%	0.085%	0.23%	0.46%
Surface		(111)	(111)	(111)	(111)	(0001)	(111)
d_z (Å)		2.49	2.48	2.52	1.89	2.19	2.21
E_b (eV)		5.14	2.89	0.095	2.37	0.6	6.38
W_M (eV)	3.07	4.92	5.54	4.22	5.44	3.5	5.47
W (eV)		3.745	3.994	3.494	4.827	3.515	4.9
COB(eV)	0.95	0.92	0.9	0.87	0.86	0.99	0.94
VOB(eV)	-0.95	-0.92	-0.92	-0.9	-0.92	-0.8	-0.94

Table 2. Mulliken charge per atomic orbital of pure material, the nearest contacted P atom and the nearest contacted metal atom, the charge transferred to/from the P atom of the Blue phosphorus, the charge transferred to/from the metal atom, and the average bond length between contacted P atoms and metal atoms.

	Charge per atomic orbital (e)	Charge of per contacted P (e)	Charge of per contacted M (e)	Charge transferred to P (e)	Charge transferred to M (e)	Bond length(Å)
Blue-P	3s 1.840 3p 3.160					
Ag	4p 0.610 4d 9.770 5s 0.620	4.944	10.991	-0.056	-0.009	2.600
Au	5p 0.680 5d 9.610 6s 0.710	5.030	10.935	0.030	-0.065	2.584
Al	3s 1.120 3p 1.880	5.082	3.163	0.082	0.163	2.519
Co	3p 0.670 3d 7.650 4s 0.680	5.105	8.949	0.105	-0.051	2.182
Sc	3p 0.920 3d 1.630 4s 0.450	4.943	2.943	-0.057	-0.057	2.628

Figure captions

Figure 1

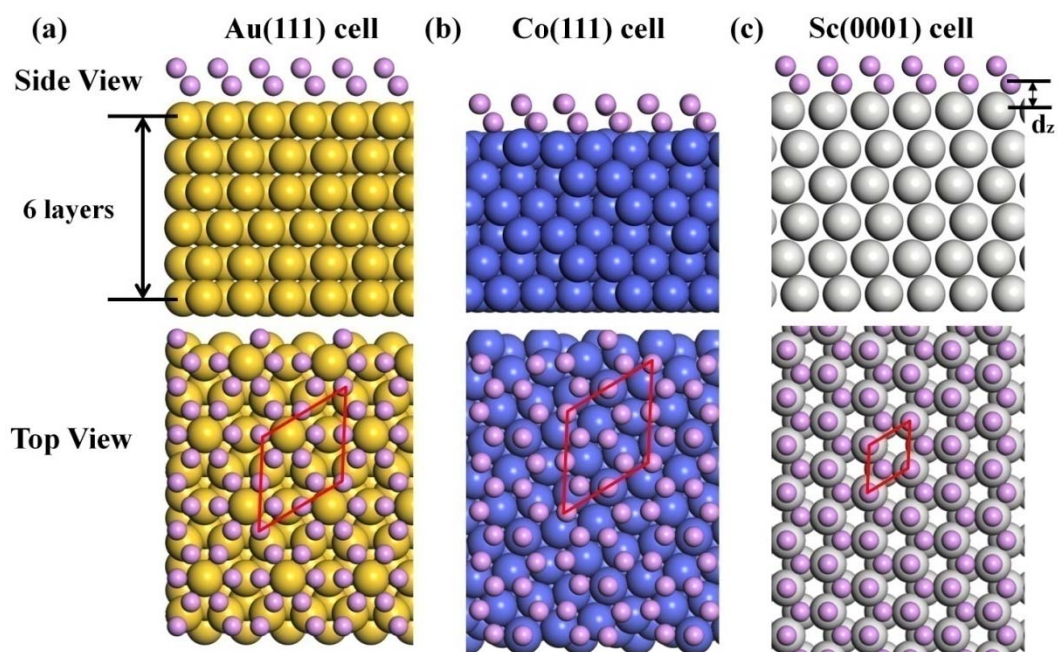


Fig.1. Atomic arrangements of BlueP on (a) Au(111), Ag(111) or Al(111) and (b) Co(111) (c) Sc(0001) surfaces.

Figure 2

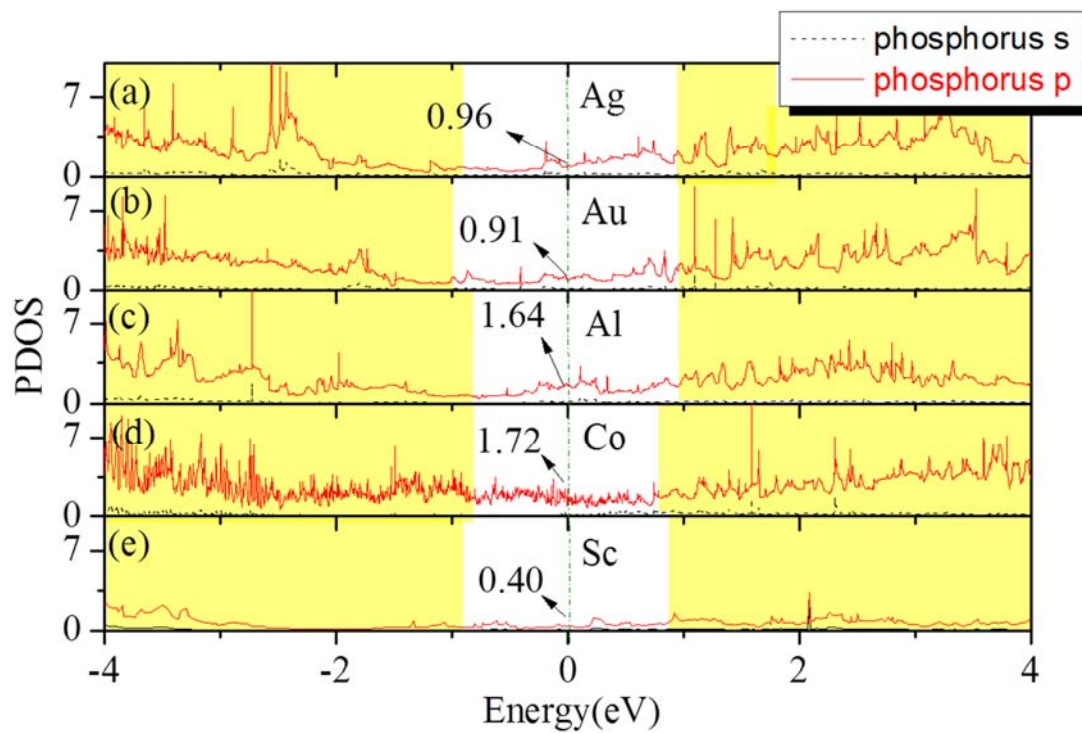


Fig.2. Partial density of states (PDOS) of P atoms, in (a) the Ag contact system, (b) the Au contact system, (c) the Al contact system, (d) the Co contact system and (e) the Sc contact system. The red solid line and the dash dot line represent p orbital, and s orbital of the monolayer P atoms as indicated by the legend in (a). The vertical green dash-dot line indicates the Fermi level for (a)–(e). The white part indicates from CBM to VBM part for (a)–(e).

Figure 3

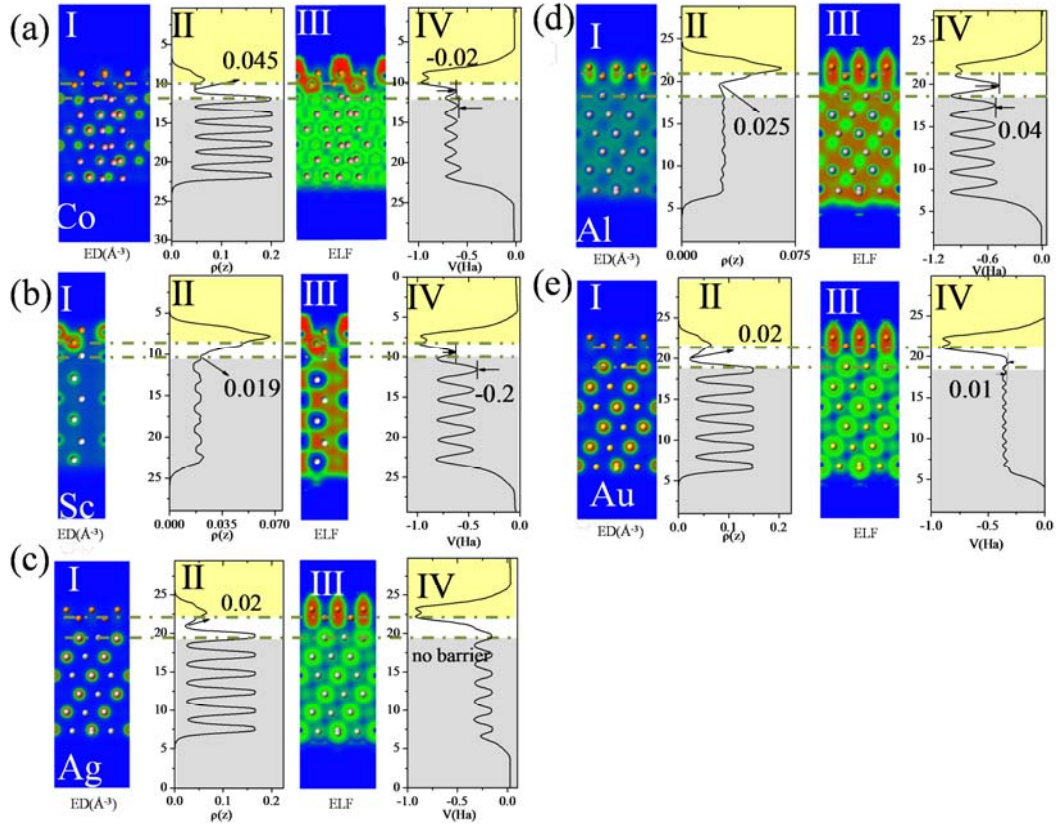


Fig. 3. Electronic properties at the interface of the contact region for (a) Co, (b) Sc, (c) Ag, (d) Al, and (e) Au substrates. The left panel (I) shows the contour plots of the charge density ρ which is integrated in the x direction [unit]. Panel (II) plots the charge density $\rho(z)$ averaged over the x and y directions. Panel (III) represents contour plots of electron localization function (ELF) which is integrated in the x direction. Panel (IV) shows the effective potential V_{eff} . The average potential barriers at the BlueP and metal interface are also indicated. In all panels, the upper green dashed lines represent the average positions of the P atoms and the lower green dashed lines represent the average positions of the metal surfaces after structure relaxation.

Figure 4

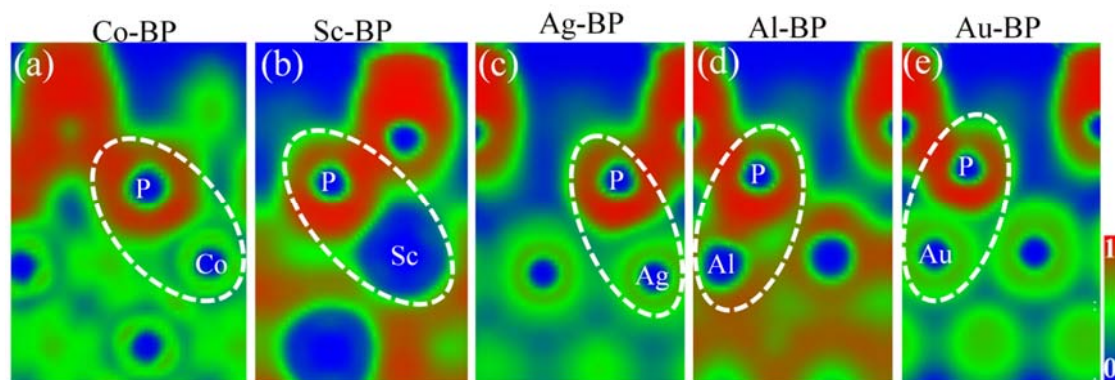


Fig. 4 The ELF of the cross-section between one phosphorus atom and its nearest metal neighbor. The color scale for (a)–(e) is shown on the right.

Figure 5

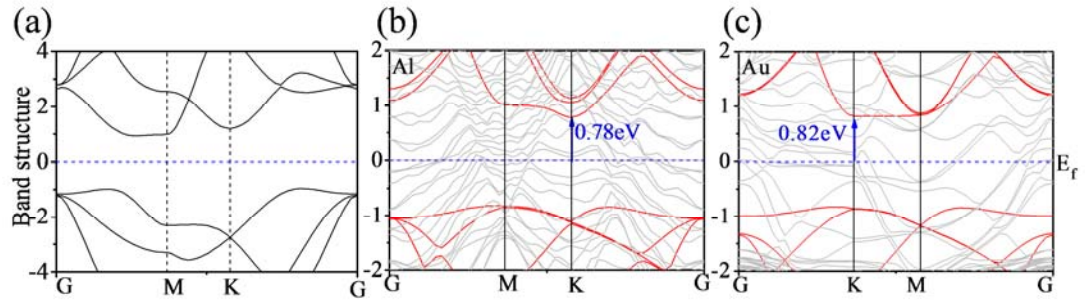


Fig. 5. Band structures of (a) freestanding BlueP (b) the Al/BlueP system, (c) the Au/BlueP system, for the mixed metal-BlueP band structure are in grey with the superimposed projected band structure of optimized original BlueP in red. The Schottky barrier (Φ_{SB}) is marked in blue.